J|A|C|S
ARTICLES
Published on Web 05/13/2006

Subunit Exchange of MjHsp16.5 Studied by Single-Molecule Imaging and Fluorescence Resonance Energy Transfer

Yinghua Guan, Zheng Wang, Aoneng Cao, Luhua Lai, and Xin Sheng Zhao*

Contribution from Beijing National Laboratory for Molecular Sciences, State Key Laboratory for Structural Chemistry of Unstable and Stable Species, and Department of Chemical Biology, College of Chemistry and Molecular Engineering, Peking University, Beijing 100871, China

Received November 2, 2005; E-mail: zhaoxs@pku.edu.cn

Abstract: MjHsp16.5 was separately labeled by fluorescent dye Cy3 and Cy5.5. The dissociation event of a single 24-mer MjHsp16.5 molecule was captured by single-molecule imaging (SMI). Temperature-regulated subunit exchange was revealed by the real-time fluorescence resonance energy transfer (FRET). The combination of single-molecular statistics and kinetic parameters from FRET experiments leads to the conclusion that below 75 °C the rate-determining step of the subunit exchange was the dissociation of the dye-labeled 24-mer in which the dimer was intact, whereas above 75 °C, smaller units emerged in the exchange and the rate-determining step had the character of a bimolecular reaction.

Introduction

Small heat shock proteins (sHsps) are abundant and ubiquitous among all organisms and have functional diversity.[1,2] The sHsps belong to a class of heat shock proteins (Hsps) that can protect proteins from thermal denaturation and irreversible aggregation under stress conditions and also have chaperone activity. According to the size, the Hsps are divided into five major families: Hsp100, Hsp90, Hsp70, Hsp60, and sHsps. The sHsps range in size from 12 to 42 K and form large oligomeric complexes of 12−42 subunits. The sHsps share a homologous α-crystalline domain with a short C-terminal extension and a variable hydrophobic N-terminal region. By exposing the hydrophobic surfaces, misfolding and partially unfolding proteins can aggregate, contributing directly to some diseases, such as cataract and Parkinson's disease[3]. Through binding non-native proteins, sHsp can suppress the aggregation and keep the proteins ready for refolding.

Due to the polydispersity, up to now only a few crystal structures of the sHsps are reported, including archeal MjHsp16.5[4] from *Methanococcus jannaschii* (living at temperature up to 94 °C[5]) and wheat sHsp16.9.[6] The quaternary structures and subunit interactions are clearly shown. Dimers are the most stable suboligomer. Although a dimer is the building block for higher assembly in both cases, their quaternary structures are different. MjHsp16.5 is a hollow spherical 24-mer, whereas sHsp16.9 is a dodecameric double disk. Some sHsps have the dimeric state.[7, 8]

The putative molecular chaperone mechanism of sHsps involves temperature-regulated exposure of hydrophobic regions that bind to exposed hydrophobic patches on protein substrates to form large sHsp−substrate complexes. Recent study on MjHsp16.5 at high temperature suggests that there is a relationship between the activation mechanism and size alteration[9,10] or subunit exchange.[11] It was proposed that the activation mechanism of MjHsp16.5 involved temperature-induced conformational change with size increment of the complex resulting in the exposure of hydrophobic substrate-binding site.[10] And even at ambient temperature, the MjHsp16.5 assemblies have loose, if not perfect, octahedral symmetry.[12] But there are different possible mechanisms to explain the chaperone activity. One is that the substrates bind to the outside surface of the sphere without the disassembly of MjHsp16.5;[9] another is that the MjHsp16.5 dissociates into smaller active subunits.[11] The subunit exchange and changes in oligomerization or in quaternary structure are suggested to be important for the sHsp activity.[13−18] Similarly, the mechanism of MjHsp16.5 subunit

(1) Saibil, H. *Curr. Opin. Struct. Biol.* **2000**, *10*, 251−258.
(2) Haslbeck, M. *Cell. Mol. Life Sci.* **2002**, *59*, 1649−1657.
(3) Clark, J. I.; Muchowski, P. J. *Curr. Opin. Struct. Biol.* **2000**, *10*, 52−59.
(4) Kim, K. K.; Kim, R.; Kim, S. H. *Nature* **1998**, *394*, 595−599.
(5) Jones, W. J.; Leigh, J. A.; Mayer, F.; Woese, C. R.; Wolfe, R. S. *Arch. Microbiol.* **1983**, *136(4)*, 254−261.
(6) van Montfort, R. L. M.; Basha, E.; Friedrich, K. L.; Slingsby, C.; Vierling, E. *Nat. Struct. Biol.* **2001**, *8*, 1025−1030.
(7) Kim, M. V.; Seit-Nebi, A. S.; Marston, S. B.; Gusev, N. B. *Biochem. Biophys. Res. Commun.* **2004**, *315*, 796−801.
(8) Bukach, O. V.; Seit-Nebi, A. S.; Marston, S. B.; Gusev, N. B. *Eur. J. Biochem.* **2004**, *271*, 291−302.
(9) Kim, R.; Lai, L. H.; Lee, H. H.; Cheong, G. W.; Kim, K. K.; Wu, Z.; Yokota, H.; Marqusee, S.; Kim, S. H. *Proc. Natl. Acad. Sci. U.S.A.* **2003**, *100*, 8151−8155.
(10) Kim, D. R.; Lee, I.; Ha, S. C.; Kim, K. K. *Biochem. Biophys. Res. Commun.* **2003**, *307*, 991−998.
(11) Bova, M. P.; Huang, Q. L.; Ding, L. L.; Horwitz, J. *J. Biol. Chem.* **2002**, *277*, 38468−38475.
(12) Haley, D. A.; Bova, M. P.; Huang, Q. L.; McHaourab, H. S.; Stewart, P. L. *J. Mol. Biol.* **2000**, *298*, 261−272.
(13) Bova, M. P.; McHaourab, H. S.; Han, Y.; Fung, B. K. K. *J. Biol. Chem.* **2000**, *275*, 1035−1042.
(14) Bova, M. P.; Ding, L. L.; Horwitz, J.; Fung, B. K. K. *J. Biol. Chem.* **1997**, *272*, 29511−29517.
(15) Giese, K. C.; Vierling, E. *J. Biol. Chem.* **2002**, *277*, 46310−46318.
(16) Koteiche, H. A.; McHaourab, H. S. *J. Biol. Chem.* **2003**, *278*, 10361−10367.
(17) Ehrnsperger, M.; Lilie, H.; Gaestel, M.; Buchner, J. *J. Biol. Chem.* **1999**, *274*, 14867−14874.
(18) Friedrich, K. L.; Giese, K. C.; Buan, N. R.; Vierling, E. *J. Biol. Chem.* **2004**, *279*, 1080−1089.

exchange has two possibilities: collision-dependent exchange and dissociation-dependent exchange.[11]

Practically, all previous knowledge has been learnt from ensemble experiments, even though the interpretation is given on a molecular level. The ensemble-averaged measurement may overlook important information that is related to the single-molecular behaviors. Recently, single-molecule imaging (SMI) has emerged as a novel tool to investigate biological processes with great details, which can provide insights into the molecular behavior and visualize the biological processes beyond the ensemble average.[19−29]

Here, for the first time, the dissociation event of 24-mer MjHsp16.5 protein was captured by SMI. As a sensitive monitor for distance, fluorescence resonance energy transfer (FRET) was employed to reveal the mechanism of subunit exchange of MjHsp16.5 in vitro at various elevated temperatures.[11] The kinetic analyses indicated that below 75°C the rate-determining step was the dissociation of the dye-labeled 24-mer, whereas above 75°C, the rate-determining step had the character of a bimolecular reaction.

Experimental Section

Expression, Purification, and Labeling. pET21a plasmid (generous gifts from Professor Sung-Hou Kim of University of California at Berkeley) containing MjHsp16.5 gene was transformed into *Escherichia coli* strain Rossetta (DE). Expression and purification of MjHsp16.5 were performed according to the reported procedure with minor modifications.[30] Following the instruction of the labeling kit (Amersham Pharmacia), the MjHsp16.5 24-mer was labeled with amine-reactive Cy3 (donor) or Cy5.5 (acceptor) separately, and the final dye/protein ratios were estimated. For the Cy3- and Cy5.5-monofunctional reactive dye, the final ratios of dye/protein assembly were 18.5 and 7.8, respectively. The concentrations of 24-mer protein were 0.52 mg/mL for Cy3−sHsp and 0.35 mg/mL for Cy5.5−sHsp. For the bisfunctional dye, the dye/assembly ratio was 11.5 for Cy3 dye. The concentrations of 24-mer protein were 0.064 mg/mL for Cy3-sHsp and 0.073 mg/mL for Cy5.5-sHsp. CD spectra indicated that the secondary and tertiary structures were probably not changed, and the size exclusion chromatography showed that there is no appreciable variation in the status of oligomerization after the labeling.[31]

Single-Molecule Imaging. A 532 nm laser beam (Millennia IIs, Spectra-Physics) was reflected by a dichroic mirror (575 nm long-pass or 560 nm long-pass filter) into a 100× objective (NA = 1.30, oil, Nikon) mounted on an inverted fluorescence microscope (TE300, Nikon).[32] The fluorescence emission from molecules was collected by the same objective and imaged onto an intensified CCD camera (I−Pentamax, Roper Scientific). Two 550 nm long-pass filters were used to block the laser scattering light. The exposure time was 50 ms per frame. To maintain total protein concentration during SMI, the dye-labeled proteins were diluted to 10^{-10} M with unlabeled proteins (10^{-7} M, 0.069 mg/ml) and were dropped onto the glass slide.

Ensemble FRET Spectrum. After the equal-volume mixture of Cy3-monofunctional dye-labeled MjHsp16.5 and Cy5.5-monofunctional dye-labeled MjHsp16.5 the solution was heated, with a heating rate of 120 °C/min by a heating/freezing stage (Linkam, THMS 600, Tadworth, UK, accuracy 0.1 K). Immediately after the solution reached the desired temperature, the fluorescence spectra excited at 514 nm were collected between 500 and 850 nm using a Renishaw Raman 1000 System (Wotton-Under-Edge, UK). The kinetic runs were taken at different temperatures. Most of the solutions were kept at each desired temperature for 90 min to reach the plateaus of the signal variation, whereas for some others, the heating time was shortened due to the fast reaction rate but no less than 30 min.

Image Analysis. The positions of the molecular trajectories were determined according to each local maximum through the movie stack. The diffusion coefficient was determined by fitting the mean-square displacements with the Enstein−Smoluchowski equation

$$\langle \Delta r^2 \rangle = 4Dt \tag{1}$$

where $\langle \Delta r^2 \rangle$ is the mean square displacement. D is the diffusion coefficient, and t is the time. In the case of dissociation into two fragments, the diffusion coefficients D_p, D_f, and D_s, representing the parent, the fast fragment, and the slow fragment, respectively, were deduced. To eliminate most uncertainties, the ratios of D_s/D_p and D_f/D_p were used as the scaled diffusion coefficients. The corresponding error in the diffusion coefficients was calculated according to the rules of error propagation.[31]

Kinetic Analysis. In the ensemble FRET experiment, the total fluorescence intensities were integrated from 500 to 850 nm for donor (Cy3) and 650 to 850 nm for acceptor (Cy5.5). The crosstalk was minimized by extracting the acceptor spectrum from the FRET spectrum using a pure Cy3 fluorophore spectrum. The FRET intensity was defined as

$$I_{\mathrm{FRET}} = \frac{I(\mathrm{Cy5.5})}{I(\mathrm{Cy3}) + I(\mathrm{Cy5.5})} \tag{2}$$

To analyze the kinetic data, we considered the increase of acceptor intensity rather than the decrease of donor intensity because of the existence of the background from non-FRET fluorescence in Cy3 due to the over labeling of Cy3. The acceptor intensity as a function of time was fit to a first-order rate equation

$$I_A(t) = A_0(1 - e^{-kt}) \tag{3}$$

or a second-order rate equation

$$I_A(t) = B_0 - \frac{B_0}{3\, e^{B_0 kt/2} - 2} \tag{4}$$

where A_0 and B_0 are fitting parameters and k is the rate constant.[31] The activation enthalpy, $\Delta H^{\ddagger}$, and activation entropy, $\Delta S^{\ddagger}$, could be derived according to the transition state theory.[33] The assumption that $\Delta H^{\ddagger}$ and $\Delta S^{\ddagger}$ were independent of temperature was made.

Results

Dissociation of MjHsp16.5 at the Single-Molecule Level. The dissociation of the parent 24-mer complex into multiple small daughter subunits was captured in solution using epi-

(19) Weiss, S. *Science* **1999**, *283*, 1676−1683.
(20) van Oijen, A. M.; Blainey, P. C.; Crampton, D. J.; Richardson, C. C.; Ellenberger, T.; Xie, X. S. *Science* **2003**, *301*, 1235−1238.
(21) Seisenberger, G.; Ried, M. U.; Endress, T.; Buning, H.; Hallek, M.; Brauchle, C. *Science* **2001**, *294*, 1929−1932.
(22) Yasuda, R.; Noji, H.; Yoshida, M.; Kinosita, K.; Itoh, H. *Nature* **2001**, *410*, 898−904.
(23) Zhuang, X. W.; Kim, H.; Pereira, M. J. B.; Babcock, H. P.; Walter, N. G.; Chu, S. *Science* **2002**, *296*, 1473−1476.
(24) Lakadamyali, M.; Rust, M. J.; Babcock, H. P.; Zhuang, X. W. *Proc. Natl. Acad. Sci. U.S.A.* **2003**, *100*, 9280−9285.
(25) Lu, H. P.; Xun, L. Y.; Xie, X. S. *Science* **1998**, *282*, 1877−1882.
(26) Bustamante, C.; Bryant, Z.; Smith, S. B. *Nature* **2003**, *421*, 423−427.
(27) Zhuang, X. W.; Bartley, L. E.; Babcock, H. P.; Russell, R.; Ha, T. J.; Herschlag, D.; Chu, S. *Science* **2000**, *288*, 2048−2051.
(28) Moerner, W. E.; Orrit, M. *Science* **1999**, *283*, 1670−1676.
(29) Peleg, G.; Ghanouni, P.; Kobilka, B. K.; Zare, R. N. *Proc. Natl. Acad. Sci. U.S.A.* **2001**, *98*, 8469−8474.
(30) Kim, K. K.; Yokota, H.; Santoso, S.; Lerner, D.; Kim, R.; Kim, S. H. *J. Struct. Biol.* **1998**, *121*, 76−80.
(31) See Supporting Information for details.
(32) Guan, Y. H.; Hong, L.; Wild, U. P.; Zhao, X. S. *Life Sci. Instrum.* **2003**, *1*, 38−39.
(33) Moore, J. W.; Pearson, R. G., *Kinetics and Mechanism*, Third ed.; John Wiley & Sons: New York, 1981; pp 197, 256.

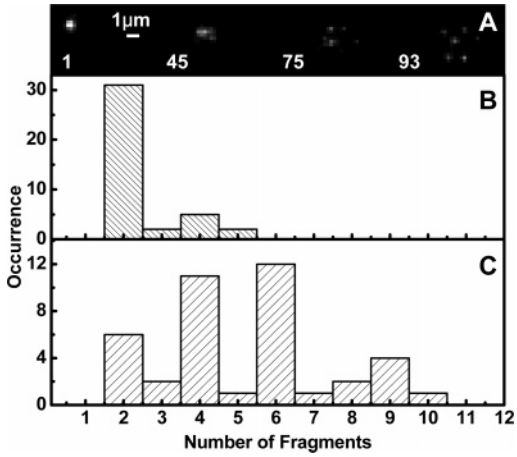

Figure 1. Dissociation of Cy3-monofunctional dye-labeled MjHsp16.5. (A) Four sequential fluorescence images show the dissociation process. As an example, this 24-mer complex dissociate into six smaller subunits. The exposure time of each frame is 50 ms, and the sequential numbers of the frames are shown. (B) The distribution of the number of fragments at the first dissociation step. (C) The final distribution of the number of fragments.

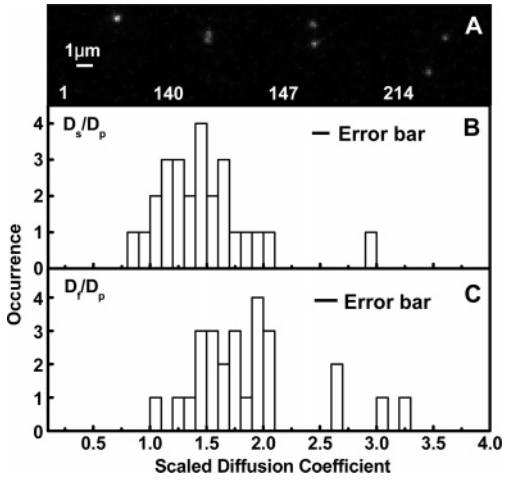

Figure 2. Cy3-bisfunctionanl dye-labeled MjHsp16.5 results in long dissociation trajectory with two fragments. (A) Fluorescence images show a two-fragment dissociation. The exposure time of each frame is 50 ms, and the sequential numbers of the frames are shown. (B) and (C) Distribution of the scaled diffusion coefficient. The error bars on the scaled diffusion coefficients are shown.

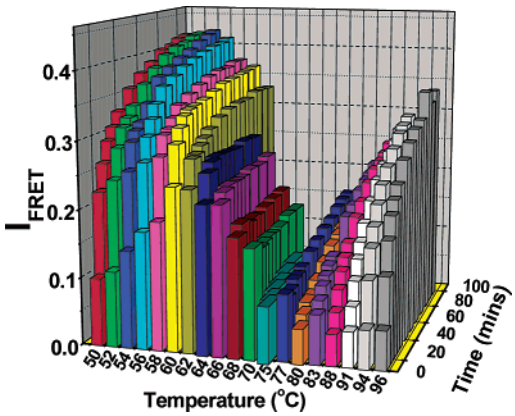

Figure 3. Ensemble reaction process monitored by FRET intensity versus time at different elevated temperatures. Obviously, three temperature regions could be recognized: the range of low temperature (50−66 °C), the range of high temperature (80−96 °C), and the range between them.

fluorescence microscope (Figure 1A). The real-time movies of disassembly are presented in the Supporting Information. The statistic analysis of 40 dissociation events showed that the process was divided into multiple steps. First, a subunit dropped from the 24-mer complex, and subsequently another one went out, one by one until the last step of dissociation finished. The 24-mer proteins could also dissociate into two fragments, and these two oligomers further dissociated into smaller fragments. Sometimes with the time resolution, the dissociation into multiple fragments could also be observed. Dominatingly, two fragments were observed in the first step of the dissociation (Figure 1B). The analysis of the final fragment number showed that there was an obvious population on even numbers (Figure 1C).

To make sure that the observed trajectories were from the dissociation process, a Cy3-bisfunctional dye was used to label the proteins with chemical cross linkage between subunits. As expected, two-fragment events were dominantly observed (Figure 2A), so that a reliable diffusion coefficient on the trajectories could be obtained. To quantitatively describe the dissociation process, the mean square displacements before and after the dissociation were calculated and fitted with the Enstein−Smoluchowski equation. Figures 2B and 2C present the distributions of the scaled diffusion coefficients. The errors in the diffusion coefficients were evaluated and are shown in the figures. Because of the reciprocal relationship between the diffusion coefficient D and the particle radius r, the scaled diffusion coefficient should be greater than one. The distributions confirmed that the observed splitting of the trajectories was due to the dissociation of the parent assembly.

To understand the mechanism of MjHsp16.5 dissociation at room temperature, we compared the observed diffusion coefficient of MjHsp16.5 with a theoretical estimation in the solution. We found that it was impossible to track the 24-mer proteins in the PBS buffer by our conditions of image collection because of the fast molecular motion. By shifting the focus point into different planes of the solution, we found that what we observed was the trajectories at the liquid−air interface. This is understandable because at the air−water interface, the proteins diffuse more slowly than that in the solution.[34,35] In our experiment, the motion of proteins could only be observed in a thin layer at the air−water interface, which means that a model of two-dimensional movement instead of three-dimensional motion should be applied. Some fast drift or directional motion was found immediately after the protein solution was dropped onto the glass slide. The two-dimensional free diffusion was imaged after 10 or 20 minutes when the solution was stable. To confirm that the observation was at the liquid−air interface, we used two glass slides to sandwich the protein solution, and we failed to capture the image of the protein motion.

Temperature-Regulated Subunit Exchange of MjHsp16.5. To determine the effect of temperature on the subunit-exchange of MjHsp16.5, we monitored the reaction through the FRET intensity over a wide range of temperatures.

Figure 3 shows the ensemble reaction processes at elevated temperatures monitored by the FRET intensity. The reaction rate increased with the temperature in 50−66 °C (the low-

(34) Sengupta, T.; Razumovsky, L.; Damodaran, S. *Langmuir* **1999**, *15*, 6991−7001.
(35) Xu, S.; Damodaran, S. *J. Colloid. Interface Sci.* **1993**, *159*, 124−133.

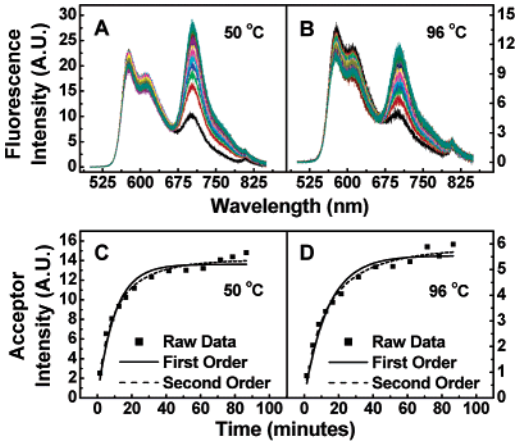

Figure 4. Time-dependent spectra of the ensemble FRET in (A) and (B) and the kinetic fit to the acceptor intensities in (C) and (D) at two representative reaction temperatures. The rate constant can be determined from the curve fit. First-order (solid line) and second-order (dashed line) reactions were used to fit the observed data (square points).

Table 1. Standard Entropy and Enthalpy of Activation Fitted with the First-Order and Second-Order Reaction-Rate Equations in Two Different Temperature Ranges

	T (°C)	$\Delta S^{\ddagger}$ (J mol^{-1} K^{-1})	$\Delta H^{\ddagger}$ (kJ mol^{-1})
First-order	50−66	226 ± 16	159 ± 5.2
	85−96	−132 ± 34	50.2 ± 12
Second-order	50−66	510 ± 16	216 ± 5.4
	85−96	−42.4 ± 46	49.6 ± 17

temperature range), but a slow process came in when the temperature was higher than 77 °C, and the reaction rate increased again with the increase of the temperature in 80−96 °C (the high-temperature range). The reaction rate in the high-temperature region was slower than the one in the lower-temperature region.

Two sets of selected data of spectra against time are shown in Figure 4A,B. Because of the uncertainty of the reaction order on the rate-determining step, the increase of the acceptor intensity was fit by the rate equations of first-order and second-order reactions, respectively. Both gave reasonable fits, as demonstrated in Figure 4C,D. $\Delta S^{\ddagger}$ and $\Delta H^{\ddagger}$ were derived (Table 1) from the Arrhenius plot (Figure 5) by using the transition state theory, assuming that both $\Delta S^{\ddagger}$ and $\Delta H^{\ddagger}$ are constants. The separate linearities in the two graphs of different temperature ranges indicate that there were two kinds of kinetic processes.

After the reaction reached a plateau at elevated temperatures, the solutions were cooled to room temperature. The final FRET intensity at the elevated temperatures and that after cooled are compared in Figure 6. The two types of profiles are obviously different. In Figure 6A, the most striking feature is the decrease of FRET intensity in the low-temperature region and the increase of FRET intensity in the high-temperature region. However, in Figure 6B, the FRET intensity continues to increase with a plateau in the major part of the low-temperature region.

Discussion

Air/Water Interface Dissociation. The mechanism of interfacial denaturation of a protein may be similar to its thermal denaturation in solution.[36,37] The inside surface of MjHsp16.5

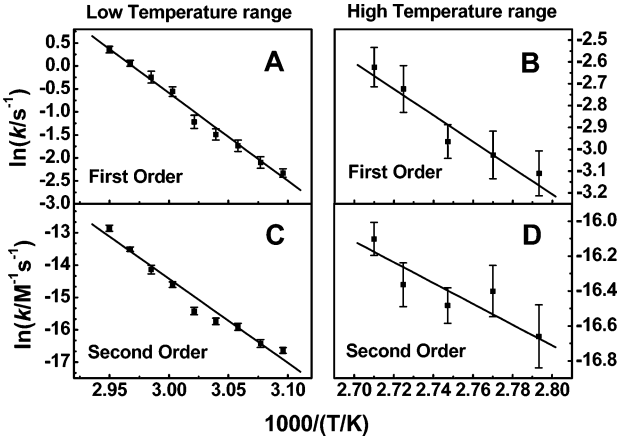

Figure 5. The plot of ln k against $1/T$ in two temperature ranges. (A) and (C): 50−66°C, (B) and (D): 85−96°C. In (A) and (B), the data (square points with error bar) are fitted (line) by the first-order rate equation, and in (C) and (D), the second-order equation is applied. From the plot, the standard entropy and enthalpy of activation can be derived.

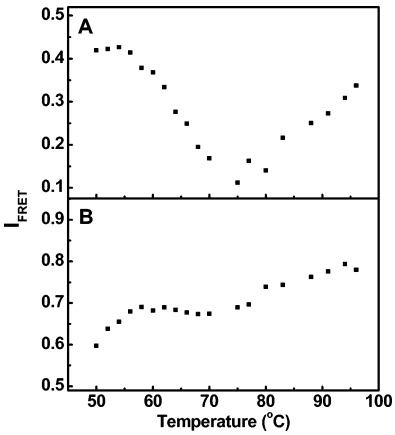

Figure 6. The comparison on the final FRET intensity at the elevated temperatures (A) and that after cooled (B). These two profiles show that the exchange mechanisms are different between the low- and high-temperature ranges.

24-mer sphere is much more hydrophobic than the outside surface, and the conserved hydrophobic residues are involved in dimer interaction.[4] When the protein is at the air−water interface, the change of its environment affects the stability of hydrogen bonding and hydrophobic and electrostatic interactions, leading to the exposure of the hydrophobic region to air and facilitating the dissociation. Water molecules will be trapped in an orderly arrangement by reorganization when the proteins denature in a solution, which causes a negative entropy change ($\Delta S = -22.4$ J mol^{-1} K^{-1} per water molecule reorganized[38]). According to the crystal structure,[4] there are in total 20 contacts around the 3-fold and 4-fold axes, including hydrogen bond, ionic interaction, and hydrophobic interaction. Therefore, the dissociation of the sHsp assembly in solution at room temperature is probably an entropy-reducing process. Opposite to the dissociation in the solution, air/water interface helps to stabilize the exposed hydrophobic domain and less water molecules are needed. So, compared with that in solutions, the interface dissociation is likely to be an entropy-driven process. Similarly,

(36) Razumovsky, L.; Damodaran, S. *Langmuir* **1999**, *15*, 1392−1399.

(37) Xu, S.; Damodaran, S. *Langmuir* **1992**, *8*, 2021−2027.

(38) Fisicaro, E.; Compari, C.; Braibanti, A. *Phys. Chem. Chem. Phys.* **2004**, *6*, 4156−4166.

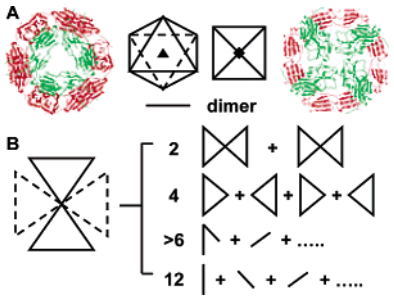

Figure 7. Schematic representation of the MjHsp16.5 protein structure with the dimer as the building block. (A) The interior of the sphere with the front one-third cut off is viewed along the crystallographic 3-fold (left) and 4-fold (right) axes. Schematic octahedrons of the structure oriented in the same way are shown in the middle. (B) The population of even-number fragments in the dissociation can be understood with the illustration.

phosphorylation may dissociate the multimeric structure to dimers.[39]

The observation on the dominant two-fragment event together with minor distribution of multiple splitting in the first step of the Cy3-monofunctional dye-labeled MjHsp16.5 proteins indicates that the observed dissociation rate is in the same order of the time resolution of the movies (50 ms/frame). The distribution of the final fragments showed even-number population in the dissociation statistics, and the maximum number is smaller than 12. There are three different dimer−dimer contacts related by the 2-, 3-, and 4-fold axes, in which the most extensive subunit contacts are found around the 2-fold axis.[4] The even-number distribution reflects the fact that the 24-mer is built on dimers with weaker contact between them (Figure 7). The ratio of 18.5 for the dye/protein assembly implies that 77% of the monomers were labeled with dyes. Therefore, it is suggested that the 24-mer complex could dissociate step by step with some final fragments being dimers.

Different Mechanisms of Subunit Exchange at Two Temperature Ranges. It is well-known that if the rate-determining step in a chemical process is a unimolecular first-order dissociation, $\Delta S^{\ddagger}$ is usually positive, because the conversion of the reactant to the transition state results in a loose molecular structure at the transition state. On the other hand, if the rate-determining step is a bimolecular second-order reaction, $\Delta S^{\ddagger}$ is usually negative, because two reactant molecules have to come together to form one transition state complex.[33] $\Delta H^{\ddagger}$ corresponds to the reaction barrier. Dissociation often has a higher $\Delta H^{\ddagger}$ than a bimolecular reaction. The comparison of the activation entropy and enthalpy at low (50−66 °C) and high (85−96 °C) temperature ranges is shown in Table 1. Regardless of the reaction order in the fitting models, the activation entropy in the low-temperature range is positive, whereas that in the high-temperature range is negative. It is also noticed that the activation enthalpy in the low-temperature range is higher than the one in the high-temperature range. Combined with the direct observation of dissociation of the 24-mer assembly in SMI, the behaviors in the two temperature ranges can be well explained by the following suggestion. In the low-temperature range, the rate-determining step is the dissociation of the 24-mer, and the subunit exchange in this low-temperature region follows the dissociation-dependent mechanism. Meanwhile, during the dissociation and subunit exchange, the dimer remains intact. When the temperature is high enough, the subunit exchange based on dimers quickly finishes; also, the higher the temperature is, the more the fragments appear. At the same time, collisions among different protein oligomers cause monomer to be exchanged between dimers, whose rate-determining step is a bimolecular reaction.

The above suggestion can also explain the results in Figure 6. From Figure 6A it is seen that the final FRET intensity reduced with the increase of temperature in the low-temperature region. This can be interpreted by that accompanying the subunit exchanges, either dissociation or expansion of the assembly proceeds with the temperature. At this moment, it is not possible for us to differentiate between the two cases. In Figure 6B, the initial increase of the FRET intensity may reflect the fact that at the moment of cooling, the exchange reaction does not reach full scale yet. The plateau in the major part of the low-temperature region indicates that after the completion of subunit exchange, the status of products at different temperatures is the same after they cooled. In the high-temperature range, the FRET intensity increases in both Figure 6A and B, which indicates that the final status is different from that in the low-temperature range. This is in agreement with the suggestion that the dimer is intact in the low-temperature range and that the exchange of monomers occurs between dimers in the high-temperature range.

At physiological temperatures, the underlying chaperone mechanism of sHsps involves the temperature-regulated exposure of hydrophobic binding sites, and their exposure is realized by the dissociation of large oligomers into smaller oligomers[6,11,14,40,41], whereas in the case of MjHsp16.5, the supportive evidence for the thermally induced expansion at elevated temperatures was provided by dynamic light scatting as well as electron microscopy.[10] The volume of the cavity of the MjHsp16.5 spherical 24-mer oligomer would not be large enough to contain 24 SCMs (single chain monellin, a model substrate) without changing the size.[42] Some other sHsps have the dissociation process under heat shock conditions.[6,40,43,44] Hsp25 16-mer complex is in a concentration-dependent equilibrium with tetramers and dimers and forms large particles when incubated above 65 °C.[17] The dissociated species expose the hydrophobic regions that are the binding site for the nonnative protein. Our observation provides some new insight regarding the mechanism of subunit exchange and protein protection.

Conclusion

In this study, for the first time, our SMI experiment has directly observed the dissociation of the MjHsp16.5 complex. The SMI results and the application of the transition state theory on FRET data have revealed different mechanisms on the temperature-regulated subunit exchange and different aggregation of MjHsp16.5 at different temperatures. Below 75 °C, the dissociation-induced subunit exchange is the dominant process in which the dimer remains intact. Above 75 °C, smaller units

(39) Lambert, H.; Charette, S. J.; Bernier, A. F.; Guimond, A.; Landry, J. *J. Biol. Chem.* **1999**, *274*, 9378−9385.
(40) Haslbeck, M.; Walke, S.; Stromer, T.; Ehrnsperger, M.; White, H. E.; Chen, S. X.; Saibil, H. R.; Buchner, J. *EMBO J.* **1999**, *18*, 6744−6751.
(41) Wintrode, P. L.; Friedrich, K. L.; Vierling, E.; Smith, J. B.; Smith, D. L. *Biochemistry* **2003**, *42*, 10667−10673.
(42) Kim, R.; Kim, K. K.; Yokota, H.; Kim, S. H. *Proc. Natl. Acad. Sci. U.S.A.* **1998**, *95*, 9129−9133.
(43) Fu, X. M.; Chang, Z. Y. *Biochem. Biophys. Res. Commun.* **2004**, *316*, 291−299.
(44) Fu, X. M.; Liu, C.; Liu, Y.; Feng, X. G.; Lu, L. C.; Chen, X. Y.; Chang, Z. Y. *Biochem. Biophys. Res. Commun.* **2003**, *310*, 412−420.

emerge in the exchange, and the rate-determining step of subunit exchange has the character of a bimolecular reaction.

Acknowledgment. X.S.Z. thanks Professor X. Sunney Xie of Harvard University for his inspiring comments and suggestions. This work was supported by NSFC (20333010, 30490172) and NKBRSF (G1999075305).

Supporting Information Available: CD spectra and size exclusion chromatography of the dye-labeled and unlabeled MjHsp16.5, the error evaluation of the diffusion coefficient, the application of the transition-state theory, and video materials of multiple splitting with a Cy3-monofuctional dye labeling and two-fragments splitting with a Cy3-bisfunctional dye labeling. This material is available free of charge via the Internet at http://pubs.acs.org.

JA057499N